One-nucleon-transfer reactions induced by 352-MeV ^{18}O on ^{28}Si

M. A. G. Fernandes, B. L. Burks, D. J. Horen, G. R. Satchler, R. L. Auble,
F. E. Bertrand, J. L. Blankenship, J. L. C. Ford, Jr., E. E. Gross,
D. C. Hensley, R. O. Sayer, D. Shapira, and T. P. Sjoreen
Oak Ridge National Laboratory, Oak Ridge, Tennessee 37831
(Received 24 February 1986)

The one-nucleon transfer reactions $^{28}Si(^{18}O,^{17}O)^{29}Si$ and $^{28}Si(^{18}O,^{19}F)^{27}Al$ have been studied at 352 MeV bombarding energy. Several strong transitions were identified in each reaction and analyzed using the distorted-wave Born approximation. A shallow, surface-transparent optical potential of E-18 type did not give acceptable results, but deeper, more conventional potentials fitted the data without any need for renormalization. Data on the same reactions taken earlier at 56 MeV were reanalyzed and the results compared to the present experiment. The use of the distorted-waves approximation is examined critically.

I. INTRODUCTION

Previous studies of one-nucleon transfer reactions between heavy ions have shown that the distorted-wave Born approximation (DWBA) frequently reproduces quite well the magnitudes of the cross sections, and the shapes of their angular distributions, for transitions to states with strong single-particle or single-hole components relative to the initial states, provided the kinematic conditions correspond to good matching between entrance and exit channels.[1] Further, it has been shown[2,3] that optical potentials that give similar elastic scattering usually yield similar transfer cross sections when used in the DWBA. However, these conclusions have been derived mainly from measurements made at low bombarding energies ($E \lesssim 10$ MeV per nucleon).

Measurements of single-nucleon transfers for $^{16}O + ^{208}Pb$ were made[3,4] for bombarding energies spanning 100–312 MeV. Although DWBA calculations correctly reproduced the relative cross sections for the different transitions at each energy, the energy dependence of their magnitudes was not reproduced. There was also a small but systematic angle shift between the measured and calculated bell-shaped angular distributions. On the other hand, a comparison[5] of single-nucleon transfers induced by $^{16}O + ^{48}Ca$ at energies of 56 and 158 MeV did not reveal a similar discrepancy. Consequently it is of interest to have more data for single-nucleon transfers at higher energies, for comparison with earlier low-energy data.

In this paper we report on a study of the neutron transfer $^{28}Si(^{18}O,^{17}O)^{29}Si$ and the proton transfer $^{28}Si(^{18}O,^{19}F)^{27}Al$ reactions at a bombarding energy of 352 MeV. The elastic and inelastic scattering in the entrance channel were measured at the same time and the results and analysis are reported separately.[6] In this paper we present a DWBA analysis of the transfer reactions, and compare the results to similar analyses of data obtained[7] at 56 MeV in order to see whether any energy dependence is present.

Experimental details are given in Sec. II and the results are shown in Sec. III. In Sec. IV we describe the DWBA calculations for both transfer reactions and the spectroscopic information derived by comparison with the measured cross sections. In particular, the results for 56 and 352 MeV are compared. Finally, Sec. V presents the conclusions of this study.

II. EXPERIMENTAL PROCEDURE

The experiment was performed using the 352 MeV beam of ^{18}O ions from the coupled tandem and cyclotron accelerators at the Holifield Heavy Ion Research Facility, (HHIRF). A self-supporting natural silicon target (92.2% ^{28}Si) with a thickness of ~ 160 $\mu g/cm^2$ was used. The typical beam intensity on target was 3–4 particle nA. The reaction products were momentum analyzed with the HHIRF broad-range spectrograph (BRS) equipped with a 38-cm-long vertical drift chamber (VDC) followed by an ionization chamber in its focal plane.[8,9] This detector system allows both position measurement and particle identification. Since the VDC also determines the angle at which the scattered particles cross the focal plane, it was possible to measure the $(^{18}O,^{17}O)$ angular distributions in 0.32 deg bins in the range $2.7° \lesssim \theta_{lab} \lesssim 10.0°$ and the $(^{18}O,^{19}F)$ data in 0.16 deg angular bins with $2.5° \lesssim \theta_{lab} \lesssim 6.7°$. An energy resolution of ~ 220 keV (FWHM) determined mostly by the target thickness was obtained.

Differential cross sections were obtained from the target thickness and integrated beam current. An estimated $\pm 10\%$ uncertainty in the absolute cross sections is due to uncertainties in the target thickness measurement and charge collection in the Faraday cup.

III. EXPERIMENTAL RESULTS

In Figs. 1 and 2 are displayed the energy spectra for the $(^{18}O,^{17}O)$ and $(^{18}O,^{19}F)$ transfers, respectively. The prominent peaks in the $(^{18}O,^{17}O)$ spectrum correspond to states in ^{29}Si that are known[10] to have substantial single-particle components, and to ^{17}O in its $\frac{5}{2}^+$ ground state. The 0.87 MeV $(\frac{1}{2}^+)$ state of ^{17}O was not populated in the present

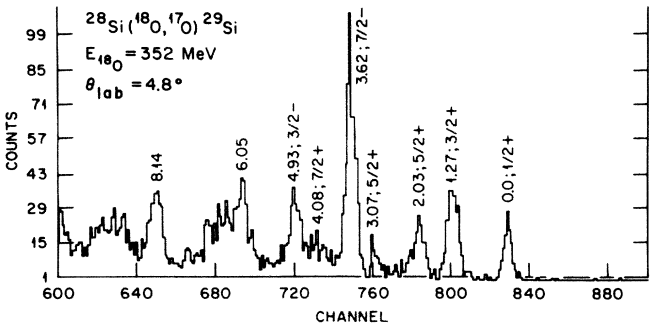

FIG. 1. The ^{28}Si(^{18}O,^{17}O)^{29}Si energy spectrum at $\theta_{lab}=4.8°$.

work, whereas at 56 MeV incident energy it was strongly excited.[7] According to DWBA calculations like those reported below, the 0.87 MeV/ground state intensity ratio is ~ 0.68 for a bombarding energy of 56 MeV, whereas at 352 MeV (with the *S*-type potential, see below) this ratio is ~ 0.09. This reduction by a factor of ~ 7.5 is sufficient to explain the absence of the groups associated with the 0.87 MeV state in the results from the present experiment.

The measured differential cross sections for the (^{18}O,^{17}O) reaction are shown in Fig. 3. Their angular distributions are almost structureless, being dominated by an exponential decrease with increasing angle. In the case of the ^{18}Si(^{18}O,^{19}F) reaction, the ^{19}F(0.199 MeV, $\frac{5}{2}^+$) state is strongly excited in comparison with the ^{19}F ground state. Such behavior is in agreement with ^{18}O(^{3}He,d)^{19}F measurements.[11] The strong groups seen in Fig. 2 represent the simultaneous excitation of the ^{19}F state at 0.199 MeV and the various predominantly single-hole states in ^{27}Al,

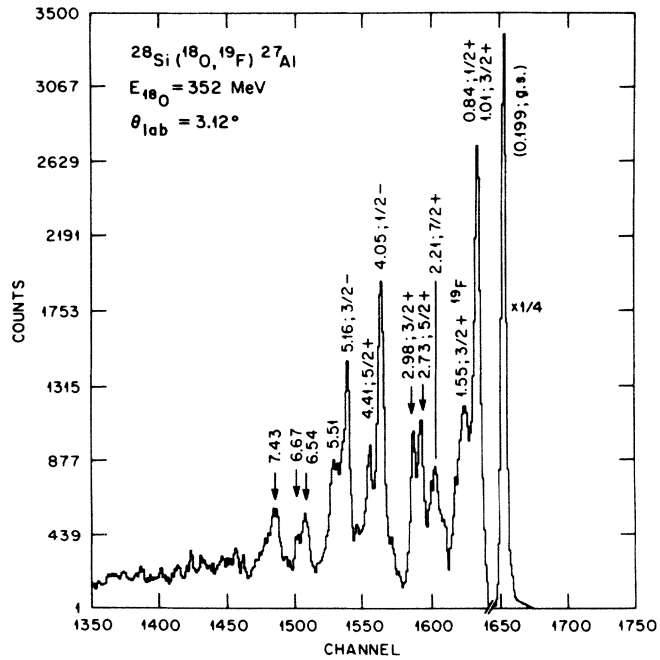

FIG. 2. The ^{28}Si(^{18}O,^{19}F)^{27}Al energy spectrum at $\theta_{lab}=3.12°$. The strong groups correspond to simultaneous excitation of the ^{19}F($\frac{5}{2}^+$,0.199 MeV) state and several strong single-hole states in ^{27}Al (see the text).

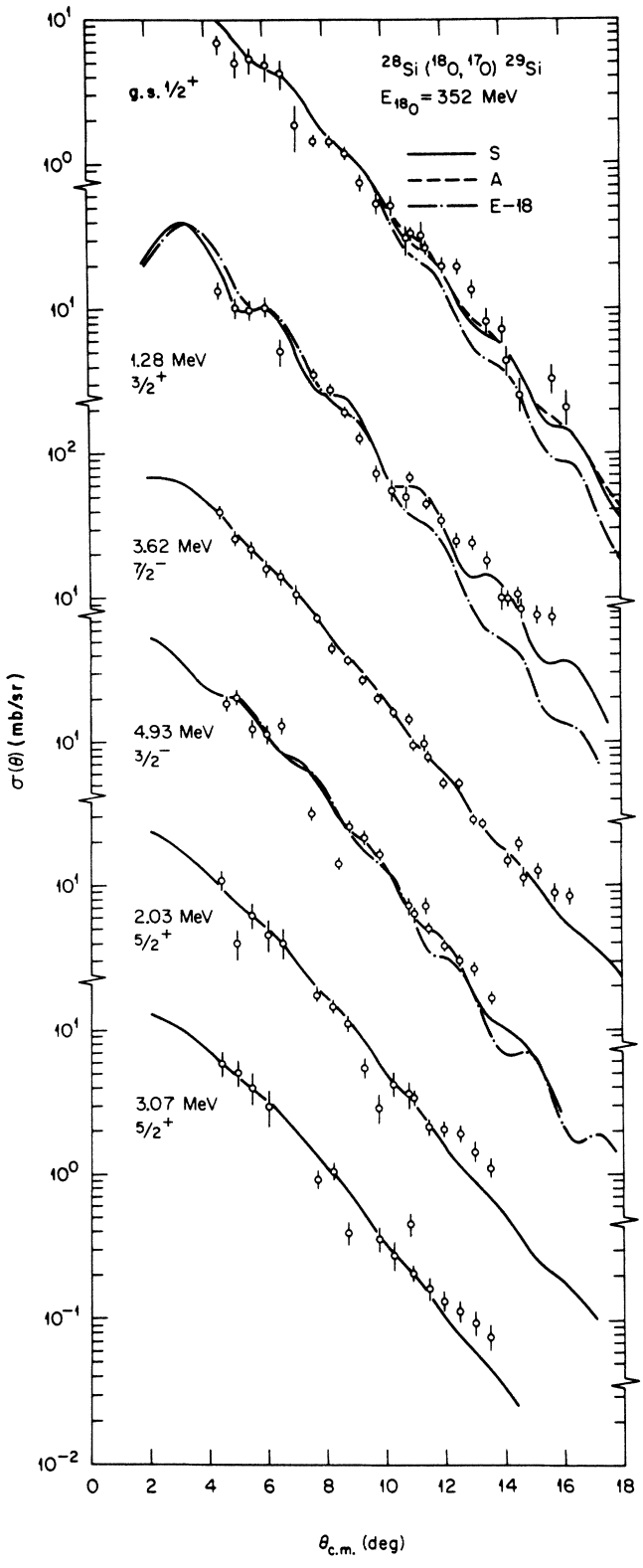

FIG. 3. ^{28}Si(^{18}O,^{17}O)^{29}Si angular distributions. The solid and dot-dashed curves are DWBA predictions using the *S* and E-18 optical potentials, respectively. For the ground-state transition the DWBA calculations using the *A* potential are also shown as a dashed curve. The corresponding normalization factors are given in Table II.

listed in the figure. In the lower energy region of some of these strong groups, it is possible to identify weak peaks corresponding to excitation of ^{27}Al states associated with ^{19}F in its ground state. The $\frac{3}{2}^+$ state of ^{19}F at 1.55 MeV excitation is also strongly populated. The ^{19}F group at 2.98 MeV excitation corresponds to an unresolved doublet consisting of the $\frac{3}{2}^+$ state at 2.97 MeV and the $\frac{9}{2}^+$ state at 3.00 MeV excitation of ^{27}Al.

Yields for individual transitions were extracted using a peak fitting procedure. The resulting differential cross sections are shown in Figs. 4 and 5. Similar to the (^{18}O, ^{17}O) case, the ^{19}F angular distributions display an exponential decrease with angle, modulated in some cases by weak oscillations.

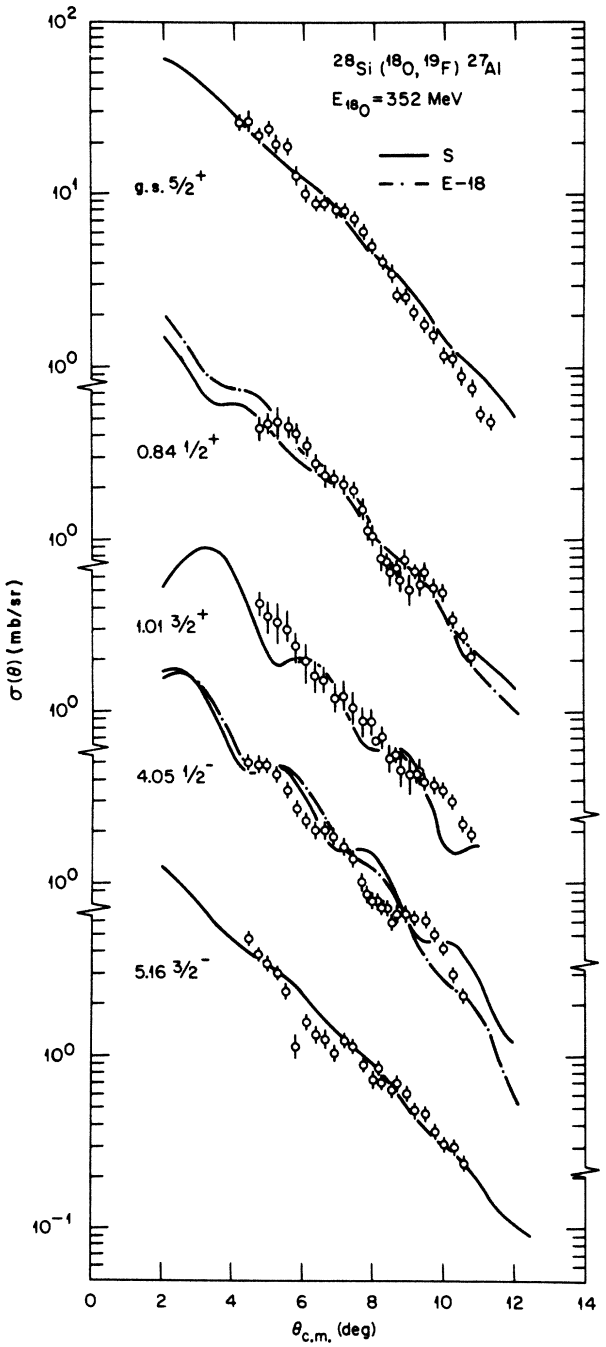

FIG. 4. ^{28}Si(^{18}O, ^{19}F)^{27}Al angular distributions. The solid and dot-dashed curves are the results of DWBA calculations using the S and E-18 potentials, respectively. The corresponding normalization factors are given in Table III.

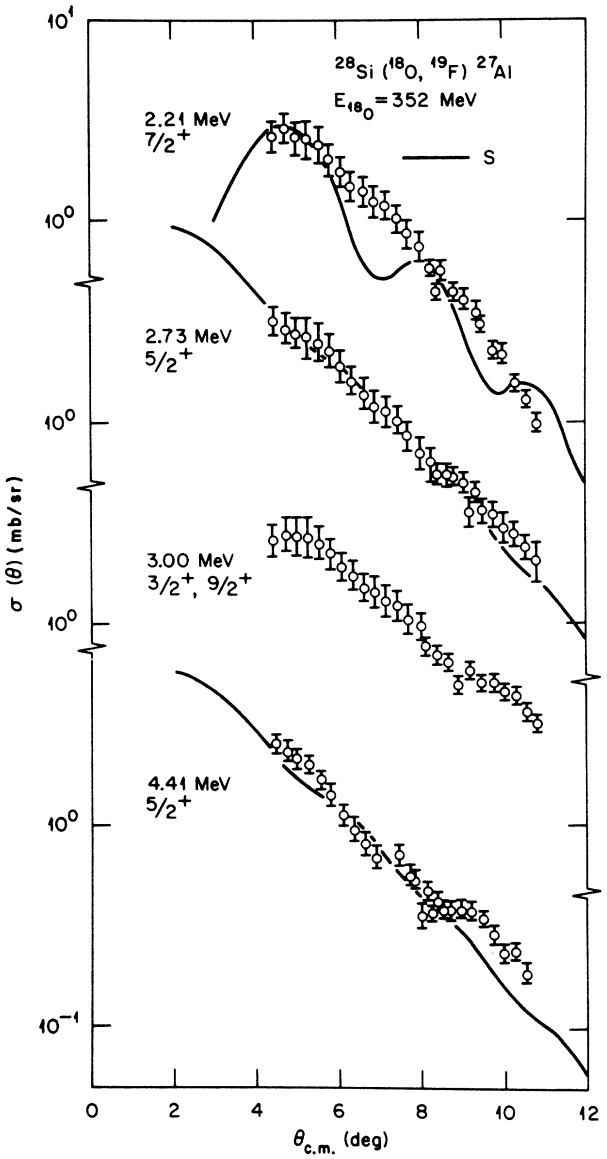

FIG. 5. ^{28}Si(^{18}O, ^{19}F)^{27}Al angular distributions. The solid curve is the result of DWBA calculations using the S potential. The corresponding normalization factors are given in Table III.

IV. DISTORTED WAVE ANALYSIS

A. The model

The heavy-ion transfer cross sections were analyzed using the usual DWBA,[1] with finite-range and recoil effects treated exactly. The earlier data[7] taken at 56 MeV were reanalyzed. The calculations were performed using the program PTOLEMY.[12] The effective interaction was chosen to be the light-ion binding potential, including the Coulomb potential for proton transfers, plus the corresponding Coulomb and (real) nuclear core interac-

TABLE I. Optical model parameters. [Standard Woods-Saxon potential, except for type F. Radii defined as $R_i = r_i(A_T^{1/3} + A_P^{1/3})$ where $i = W$, v, or c. Coulomb potential for a point charge incident upon a uniform charge distribution of radius R_c. See Ref. 6 for details.]

Type	Energy (MeV)	V (MeV)	r_v (fm)	a_v (MeV)	W (fm)	r_W (fm)	a_W (fm)	r_c (fm)
A	352	100	0.971	0.652	44.1	1.043	1.051	1.3
S	352	50	1.077	0.641	43.0	1.041	1.004	1.077
E-18	352	10	1.291	0.725	23.4	1.191	0.599	1.0
S	56	50	1.093	0.743	43.0	1.093	0.743	1.093
E-18	56	10	1.383	0.571	23.4	1.200	0.709	1.0
F[a]	352	141.3	1.0	1.23	251.7	0.7	0.977	1.3

[a]Imaginary part is Woods-Saxon, but the real part is the square of a Woods-Saxon potential.

tions.[1,12–14] The nucleon binding potentials were taken to be of the usual Woods-Saxon form, with their depths adjusted to give the experimental separation energies. The choice of the other parameters for these potentials is discussed in the next subsection.

The optical potentials for the distorted waves in the entrance channel were obtained by analyzing the elastic scattering data;[6,7] the parameters are listed in Table I. These data do not yield unique potentials, and we explored the consequences of these ambiguities for the predicted transfer cross sections. The optical potentials for the exit channels were assumed to be the same as for the entrance channel; such a choice appears to be justified by the results of other studies.[2,15] For the real potential both Woods-Saxon and Woods-Saxon-squared potential forms were used. The parameters of the real part of the latter (F in Table I) were chosen to reproduce the shape of a folded potential[6] in the important radial region of $r \approx 5-12$ fm. The folded potential gives a good account of the elastic data[7] at 56 MeV, and at similar low energies,[16] without any need for renormalization, but its strength had to be reduced by a factor of almost 2 in order to fit the elastic data at 352 MeV. The optical model analyses have some general implications for the transfer reactions, and these are discussed in Sec. IV D below.

Because both target and projectile have zero spin in the present case, only one shell model orbital in either nucleus can contribute to the excitation of a given final state, so each transition is characterized by the transfer of the nucleon from the initial l_1, j_1 to the final l_2, j_2 shell model quantum numbers. Associated with each of these orbitals l,j is the corresponding spectroscopic factor[1] $\tilde{S}_{lj} = C^2 S_{lj}$ for that transition. These are normalized such that for pickup from the l,j orbital we have $\tilde{S}_{lj} \leq 2j+1$, and for stripping into the l,j orbital $\tilde{S}_{lj} \leq 1$. Further, for a spin-zero target nucleus there are the sum rules:[1]

$$\sum_f \tilde{S}_{lj}^f = n(l,j): \text{ pickup}, \tag{1a}$$

$$\sum_f \tilde{S}_{lj}^f (2j+1) = (2j+1) n(l,j): \text{ stripping}, \tag{1b}$$

where the sum is over final states f, and $n(l,j)$ is the occupancy of the l,j orbit in the target nucleus.

The resulting differential cross section for each transition then can be written in the form

$$d\sigma/d\Omega = N \tilde{S}_{l_1 j_1} \tilde{S}_{l_2 j_2} \sigma^{\mathrm{DW}}_{l_1 j_1 l_2 j_2}(\theta), \tag{2}$$

where σ^{DW} is the cross section calculated in DWBA (assuming each $\tilde{S} = 1$) and N is an overall normalization factor. If the DWBA is an accurate description of the process, and the various parameter values have been chosen correctly, we should have $N = 1$. The curves shown in Figs. 3–5 represent the calculated cross sections; the corresponding values of the quantities N, $\tilde{S}_p = \tilde{S}_{l_1 j_1}$, and $\tilde{S}_t = \tilde{S}_{l_2 j_2}$ are given in Tables II and III. The quantities $\tilde{S}_p$ and $\tilde{S}_t$ refer to the spectroscopic factors for the light and heavy system, respectively. No values associated with potential F are listed in these tables. For both (^{18}O,^{17}O) and (^{18}O,^{19}F) transitions, the DWBA cross sections obtained with this potential are $\simeq 10-12\%$ ($\simeq 45\%$) larger than the theoretical predictions with the $S(A)$ potential.

B. Nucleon binding potentials, and spectroscopic factors from light-ion reactions

The choice of parameters for the Woods-Saxon potentials that bind the nucleon before and after its transfer has negligible effects on the shape of the angular distributions and on the *relative* cross sections to different final states, but it can have dramatic effects on the absolute magnitude of the cross sections. Consequently, the absolute magnitudes of the spectroscopic factors deduced from the measurements can depend sensitively upon this choice. Hence it is important to obtain, if possible, some independent justification for the parameters used. For this we can appeal to the results of analyses of direct transfer reactions using light ions. Each of these is subject to its own uncertainties, of course. We also note that the use of a Woods-Saxon form is only an approximation,[1] so that in principle different parameter values could be appropriate for different orbitals. We do not make use of this additional freedom.

For reference, and to facilitate comparison with the results of analyses of other heavy-ion experiments,[7,15] we adopt a standard set of parameters:

$$r_0 = 1.20 \text{ fm}, \quad a = 0.65 \text{ fm}, \quad V_{\mathrm{so}} = 7 \text{ MeV}, \tag{3}$$

where the real well depth V is adjusted to give the observed separation energy for each transition and the spin-orbit term uses the same r_0 and a as the central term. The potential radii are defined as $R = r_0 A_c^{1/3}$, where A_c is the mass number of the core to which the nucleon is bound in the $A_c + 1$ system. For the protons we add the

TABLE II. Neutron spectroscopic factors for $^{28}Si \rightarrow {}^{29}Si$. [The first number is for the relative normalization factor $(N\tilde{S}_p\tilde{S}_l)/(N\tilde{S}_p\tilde{S}_l)_{g.s.}$. The number in parentheses is for $\tilde{S}_l$, assuming $N=1$ and $\tilde{S}_p=1.6$ for (^{18}O, ^{17}O) or $\tilde{S}_p=2.0$ for (^{15}N, ^{14}N).]

		(^{18}O, ^{17}O)				(d,p)[a]	(^{15}N, ^{14}N)[b]	
		$E=351.7$ MeV[d]		$E=56$ MeV[e]		$E=18$ MeV	$E=44$ MeV	
Potential[f]	A	S	E-18	S	E-18		E-18	Shell model[c]
Level								
g.s. $\frac{1}{2}^+$	1.0(0.81)	1.0(0.66)	1.0(0.28)	1.0(0.66)	1.0(0.67)	1.0(0.58)	1.0(0.60–0.59)	1.0(0.50)
1.28 MeV $\frac{3}{2}^+$	1.37(1.11)	1.38(0.91)	1.18(0.33)	2.36(1.56)	2.56(1.72)	1.40(0.81)	1.83–2.03(1.09–1.19)	1.2(0.59)
2.03 MeV $\frac{5}{2}^+$	0.23(0.19)	0.26(0.17)				0.23(0.13)	0.24–0.28(0.15–0.16)	0.22(0.11)
3.07 MeV $\frac{5}{2}^+$	0.15(0.12)	0.15(0.10)				0.11(0.07)	0.10(0.06)	0.04(0.02)
3.62 MeV $\frac{7}{2}^-$	0.56(0.45)	0.61(0.40)		0.86(0.57)	0.90(0.60)	0.75(0.44)	0.77–0.94(0.46–0.55)	
4.93 MeV[g] $\frac{3}{2}^-$	0.95(0.77)	1.01(0.67)	0.94(0.26)	0.77(0.51)	0.79(0.53)	1.04(0.60)		

[a]Reference 10. The $\tilde{S}_l$ values have been increased by 10% to correspond to a binding potential with $r_0=1.20$ fm: see the text.
[b]Reference 15. The two values correspond to different choices for the exit-channel potential.
[c]Reference 20.
[d]Present experiment.
[e]Reanalysis of data from Ref. 7.
[f]See Table I.
[g]A $2p_{3/2}$ orbital was assumed.

Coulomb potential from a uniform charge with radius parameter $r_c=1.20$ fm.

Information on the $^{18}O=^{17}O+n$ system is available from analysis[17] of $^{17}O(d,p)^{18}O$ measurements. A ground state ($1d_{5/2}$) spectroscopic factor $\tilde{S}=1.22$ was obtained when using $r_0=1.25$ fm. This is somewhat smaller than the theoretically expected[18] value of about 1.6. The discrepancy would be reduced if our standard $r_0=1.20$ fm were used; we conclude that the standard parameter set in Eq. (3) is probably satisfactory in this case.

For the $^{18}O+p \rightarrow {}^{19}F$ transitions we have analyses[11] of $^{18}O(^3He,d)$ reactions measured at incident energies of 11 and 16 MeV. The former yielded $\tilde{S}=0.42$ for the 0.199 MeV $\frac{5}{2}^+$ state in ^{19}F that is observed in the present work, when using $r_0=1.25$ fm together with a nonlocality correction that we do not consider here. Exclusion of this correction and use of our standard $r_0=1.20$ fm would probably have increased this spectroscopic factor to about 0.5. The analysis of the 16 MeV experiment gave $\tilde{S}=0.41$ for this transition; unfortunately the bound state parameters used were not given. The theoretically predicted spectroscopic factor[18] for this transition is $\tilde{S}\approx 0.4$–0.5, so again our standard set of parameters would seem to be reasonable.

The addition of a neutron to ^{28}Si has been studied[10] using the $^{28}Si(d,p)$ reaction. The analysis used the zero-range form of the DWBA with $r_0=1.25$ fm. Calculations for other systems[19] imply that the spectroscopic factors would be increased by about 10% if $r_0=1.20$ fm had been used. Hence, the absolute values of the $\tilde{S}$ listed in Table II for the (d,p) reaction have been increased by 10% over those from Ref. 10 in order to correspond to our standard set of potential parameters given in Eq. (3). The $\tilde{S}$ values for the ground and first excited states are then somewhat larger than those predicted[20] (0.5 and 0.6, respectively), but still within the uncertainties of such analyses. Further, the shell model calculations[20] were done within a restricted basis.

Proton pickup from ^{28}Si was measured[21,22] using the $^{28}Si(d,^3He)^{27}Al$ reaction. The spectroscopic factors, listed in Table III, were obtained using the zero-range DWBA and the standard set of binding potential parameters with $r_0=1.20$ fm. The ratio of the $\tilde{S}$ values from the two measurements ranges from 0.6 for the ground state of ^{27}Al to 1.2 for the first excited state, but is within 10% of unity for the two other strongly excited states. The theoretically predicted[20] values fall between the two "measured" values for both the ground and first excited states. Within these uncertainties, the standard set of parameters with $r_0=1.20$ fm appears to be satisfactory.

An additional uncertainty occurs[21] for pickup from ^{28}Si leading to the negative parity states $\frac{1}{2}^-$ and $\frac{3}{2}^-$. One interpretation is pickup from the $1p$ shell. Another is $2p$ pickup from two-particle, two-hole admixtures of the form $(2s,1d)^4(2p)^2$ in the ^{28}Si ground state. For a given binding energy, the $2p$ wave function has a larger radial extent, and requires a much smaller spectroscopic factor to match the observed cross section [a factor of 4 in the case[21] of the ($d,^3He$) reaction]. However, both the $1p$ hole and the $2p$ particle centroids would be expected to be at an excitation of 14 MeV or so. Hence the components

TABLE III. Proton spectroscopic factors for $^{28}Si \rightarrow {}^{27}Al$. [The first number is for the relative normalization factor $(NS_pS_t)/(NS_pS_t)_{g.s.}$. The number in parentheses is for $\tilde{S}_t$, assuming $N=1$ and $\tilde{S}_p=0.41$ for (^{18}O,^{19}F).]

Potential		$(^{18}O,{}^{19}F)$[a] $E=351.7$ MeV			$(d,{}^3He)$[b] $E=34$ MeV	$(^{15}N,{}^{16}O)$[c] $E=44$ MeV	
	A	S	E-18			E-18	Shell model[d]
Level							
g.s. $\frac{5}{2}^+$	1.0(4.17)	1.0(3.42)	1.0(1.25)		1.0(3.76)	1.0	1.0(3.5)
0.84 MeV $\frac{1}{2}^+$	0.17(0.70)	0.16(0.55)	0.16(0.20)		0.13(0.49)	0.27	0.16(0.55)
1.01 MeV $\frac{3}{2}^+$	0.27(1.12)	0.28(0.97)			0.15(0.56)	0.27	0.01(0.03)
2.21 MeV $\frac{7}{2}^+$	0.27(1.11)	0.32(1.11)	0.21(0.26)		(≤ 0.4)		
2.73 MeV $\frac{5}{2}^+$	0.21(0.87)	0.20(0.68)			0.16(0.61)		
4.05 MeV[e] $\frac{1}{2}^-$	0.62(2.57)	0.59(2.00)	0.48(0.60)		0.48(1.80)		
	0.09(0.38)	0.08(0.29)	0.08(0.10)		0.11(0.43)		
4.41 MeV $\frac{5}{2}^+$	0.17(0.70)	0.17(0.58)			0.09(0.35)		0.02(0.06)
5.16 MeV[e] $\frac{3}{2}^-$	0.35(1.45)	0.33(1.2)	0.26(0.32)		0.27(1.0)		
	0.10(0.41)	0.09(0.32)	0.08(0.10)		0.06(0.24)		

[a]Present experiment.
[b]Reference 21.
[c]Reference 15. Obtained with optical potentials that do not fit the elastic scattering.
[d]Reference 20.
[e]The first line corresponds to use of a $1p$ orbital, the second line to a $2p$ orbital.

found at low excitation have been displaced far from their zero-order position. More realistic transfer form factors[1] could be regarded as a linear combination of $1p$ and $2p$ components whose precise shapes and magnitudes depend upon the details of the nuclear structure involved. This situation is analogous to that encountered for neutron stripping to the $\frac{3}{2}^+$ state at 2.02 MeV in ^{41}Ca, for which more realistic form factors were constructed explicitly.[23]

An independent source of information on the protons within ^{28}Si is provided by an analysis[24] of electron scattering from ^{28}Si using a shell model density distribution. This required a Woods-Saxon potential for the protons with $r_0=1.325$ fm, $a=0.72$ fm and occupancies of $n(2s_{1/2})=0.9$, $n(1d_{5/2})=5.1$. These occupancies are comparable to those obtained from the $(d,{}^3He)$ measurements.[21,22] Since center-of-mass recoil effects were included explicitly, these shell model wave functions should also be appropriate[1] for use in transfer calculations. However, the use of such large r_0 and a values in analyses of the $(d,{}^3He)$ data would yield appreciably smaller spectroscopic factors, since it was reported[21] that the smaller increase of r_0 from 1.20 to 1.25 fm already reduces the spectroscopic factors by 20%. Such small values of $\tilde{S}$ would seem to be incompatible with the predictions of the shell model.[20] The use of these parameter values in calculations of the heavy-ion-induced transfer has similarly dramatic effects. Typically the cross sections at 352 MeV are increased by factors of about 1.6 to 1.7 for neutron transfer, and 2 or greater for proton transfer, compared to those obtained using the standard set. This corresponds to spectroscopic factors smaller by 40% to 50%. Similar results are obtained at the lower energy of 56 MeV.

In summary, the results of light-ion measurements, compared to the spectroscopic factor values suggested by shell model calculations, for the same pickup or stripping transitions studied in the present work, indicate that the standard parameter set (with $r_0=1.20$ fm) for the binding potentials is a reasonable choice. However, as the preceding discussion shows, there are appreciable uncertainties.

C. Angular momentum transfers

The resultant orbital angular momentum transfer l between the two nuclei for a transition $l_1,j_1 \rightarrow l_2,j_2$ has allowed values determined by the conditions,

$$|l_1-l_2| \leq l \leq l_1+l_2 , \tag{4a}$$

$$|j_1-j_2| \leq l \leq j_1+j_2 . \tag{4b}$$

These various l values contribute incoherently to the cross section,

$$\sigma^{DW}_{l_1j_1l_2j_2}(\theta)=\sum_l \sigma_{l;l_1j_1l_2j_2}(\theta) . \tag{5}$$

The angular distribution is largely determined by the values of l; when more than one value contributes, their sum may wash out any oscillatory structure in the angular distributions for individual l transfers.[14] Figure 6 shows the various l components for the neutron transfers to the $\frac{3}{2}^-$ state at 4.93 MeV and the $\frac{3}{2}^+$ state at 1.28 MeV in ^{29}Si at a bombarding energy of 352 MeV. The qualitative features are independent of the optical potentials used. Other transitions exhibit similar behavior, except that the amplitudes of the oscillations may vary. For example, the ground state neutron transfer (to the $2s_{1/2}$ orbit) has uniquely $l=2$, but Fig. 3 shows that its angular distribution has very little structure. In contrast, Fig. 6(b) shows that all l components, including $l=2$, for transfer into the $1d_{3/2}$ orbit show considerable oscillations.

The natural parity components (those with $l+l_1+l_2=$even, or $l=2$ and 4 here) oscillate approximately in phase with each other, except at the most forward angles ($\theta_{c.m.}<4°$). The unnatural parity terms ($l=1$

and 3) also oscillate in phase with each other, but out of phase with the natural parity ones, in the same angular range. The sum (Fig. 3) shows considerably less structure than the individual components. Also noteworthy is the fact that, at 352 MeV, the unnatural parity contributions are comparable to the natural parity ones, whereas at 56 MeV they represent $\lesssim 10\%$ and the largest contribution is obtained from the largest angular momentum transfer for each transition. These unnatural parity terms would have vanished in a theory that neglected recoil.

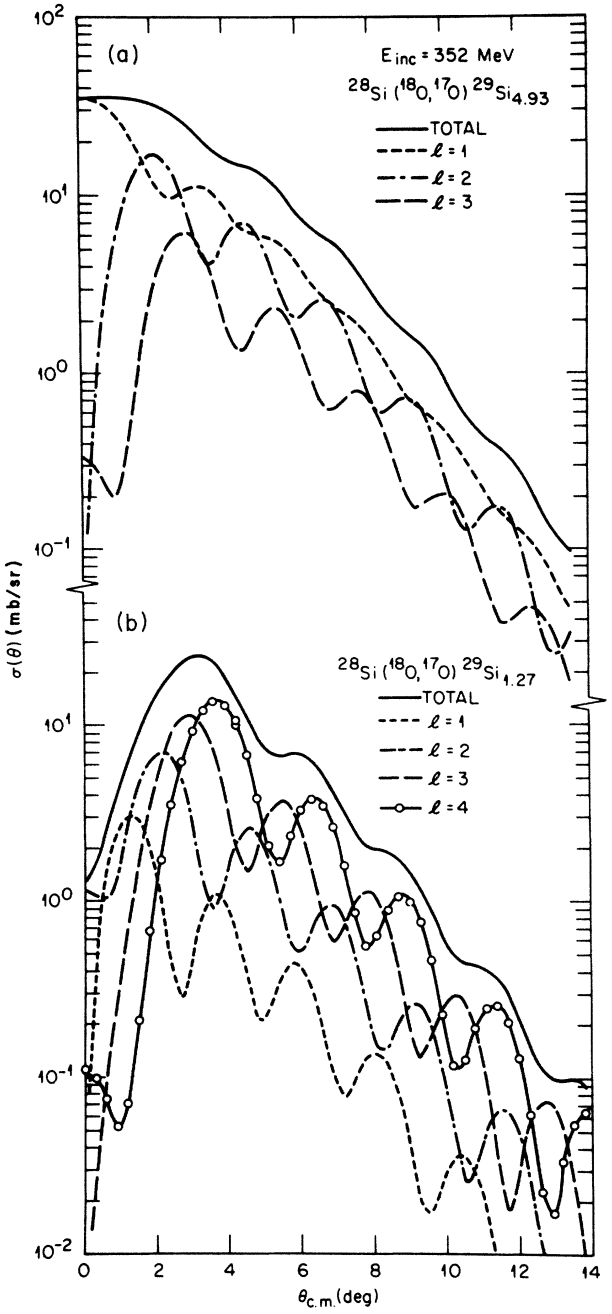

FIG. 6. Decomposition of DWBA neutron transfer cross sections at 352 MeV into incoherent contributions from transfers of various angular momenta l. (a) $2p_{3/2}$ capture into the 4.93 MeV state of ^{29}Si; (b) $1d_{3/2}$ capture into the 1.27 MeV state of ^{29}Si. The A-type optical potential was used.

The smallest l transfer, $l=1$, dominates for the transition to the $p_{3/2}$ orbital shown in Fig. 6(a), whereas the largest ($l=4$) dominates for neutron transfer to the $d_{3/2}$ orbital. This occurs because there is very little probability of the nucleon spin being reoriented during the transfer.[25] Then for grazing collisions the transition $j_1=l_1+\frac{1}{2} \rightarrow j_2=l_2+\frac{1}{2}$ favors the transfer $l=|l_1-l_2|$, while $j_1=l_1+\frac{1}{2}\rightarrow j_2=l_2-\frac{1}{2}$ favors $l=l_1+l_2$.

D. Relation between elastic scattering and transfer reactions

In this section we discuss the degree of localization of the reaction process, both in radius and in the relative orbital angular momentum L, in relation to the S-matrix elements obtained from the optical model analyses of the elastic scattering.[6]

First, however, we note that a near-side–far-side decomposition[6] of the elastic scattering at 352 MeV showed the near side scattering to be dominant over the whole angular range for the E-18 type of potential, and for $\theta_{\text{c.m.}} \lesssim 20°$ in the case of the deeper potentials, although the far side component was large enough to produce an oscillatory interference pattern even for $\theta_{\text{c.m.}} < 20°$. Similar results are expected from a far-side–near-side analysis of the transfer reactions.[26] However the present transfer data are confined to the forward angles $4° \lesssim \theta_{\text{c.m.}} \lesssim 14°$ where the near side scattering is dominant although again the far side amplitude is large enough even in this range to provide the interference oscillations seen in Fig. 6. It would be necessary to have transfer data for $\theta_{\text{c.m.}}$ greater than 20°, where the far-side–near-side crossover occurs for the deeper optical potentials,[6] before any clear distinction between the various optical potentials could be made. These cross sections would be very small. There is no indication of true rainbow effects in the elastic scattering, so none would be expected for the transfer cross sections.

Figure 7 shows one example of the distribution of contributions to the transfer at $E=352$ MeV from various partial waves L. Each DWBA cross section in Eq. (5) has the form

$$\sigma_l^{\text{DW}}(\theta) \alpha \sum_m \left| \sum_{LL'} \alpha_{LL'l}^m(\theta) I_{LL'l} \right|^2 , \tag{6}$$

where $\alpha(\theta)$ is a "geometrical" factor and the $I_{LL'l}$ are radial integrals. Plotted in Fig. 7 are the radial integrals[12] $I_{LL'l}$ with $L'=L$ and $l=2$; other terms with $L' \neq L$, and those for other l and for other transitions, all show very similar behavior.

The elastic S-matrix elements at $E=352$ MeV are essentially zero, $|S_L| \approx 0$, for $L \lesssim 60$, due to absorption. The effect of absorption on the DWBA integrals can be represented approximately by

$$I_{LL'l} \alpha (|S_L| \, |S_{L'}|)^{1/2} . \tag{7}$$

This accounts for the cutoff in $I_{LL'l}$ for values of $L \lesssim 60$. The distance of closest approach along a classical trajectory[27] with $L=60$ ranges from 5.6 fm for the type-A optical potential to 6.0 fm for the E-18 type of potential. (It is 6.1 fm for a Rutherford trajectory.) For comparison,

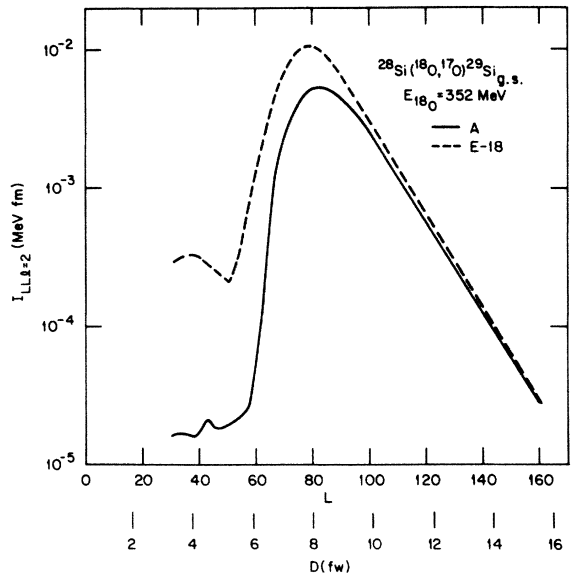

FIG. 7. The distribution of the partial-wave $I_{LL'l}$ radial integrals with $L'=L$ and $l=2$ for the ground-state neutron transfer at 352 MeV obtained from DWBA calculations using either A (solid) or E-18 (dashed) type of optical potentials. Also included is a scale of the distance of closest approach D for Rutherford trajectories in the entrance channel with angular momentum L.

the sum of the half-density radii for ^{18}O and ^{28}Si is about 5.9 fm. No significant contribution to the transfer comes from closer collisions.

The $|S_L|$ approach unity for large L values ($L \gtrsim 120$). Only Coulomb distortion is present for these partial waves, so that the $I_{LL'l}$ for different optical potentials converge to the same values, as the example in Fig. 7 demonstrates. The exponential decay with increasing L is due to the exponential decay of the bound state wave functions for the transferred nucleon.

The "strong absorption" L values, for which $d|S_L|/dL$ is a maximum, range[6] from $L_F \approx 76$ for the E-18 type of potential to $L_F \approx 81$ for the A-type potential. This is also a measure of the partial waves which contribute most to peripheral reaction processes,[28] in agreement with the maxima of the $|I_{LLl}|$ distributions shown in Fig. 7. However, the distorted waves from the A-type potential are more strongly absorbed for these partial waves than are those from the surface-transparent E-18 type; the $|S_L|$ for $L \approx L_F$ are twice as large for the latter potential. We see from Fig. 7 that this is true also for the I_{LLl}, in accordance with Eq. (7). This explains why the DWBA cross sections calculated with the E-18 type of potential are between three and four times larger than those obtained with the A-type of potential (see Tables II and III).

The classical trajectories[27] with angular momentum $L \approx L_F$ have distances of closest approach of about 8 fm. Because the exponential decay of the bound state wave functions inhibits transfer for larger separations, this means that the transfer is most likely to occur at this distance also, when the half-density points of the two nuclei are separated by about 2 fm.

A similar study was made of the calculations for a bombarding energy of 56 MeV. A strong absorption $L_F \approx 25$ is obtained for both types of optical potential, with the corresponding $|S_{L_F}|$ differing by only a few percent. Correspondingly, the DWBA transfer cross sections were found to be very similar in magnitude, while again the radial integrals were largest for $L \approx L_F$. Now the distance of closest approach for the classical trajectory with $L=L_F$ is nearly 9 fm, indicating that the reaction region at 56 MeV has moved out about 1 fm compared to that at the higher energy.

E. Uncertainties in the analyses

Already one has assumed that the DWBA provides an adequate description of the transition; we do not know how to ascribe an uncertainty to the extracted values of the product $(N\tilde{S}_p\tilde{S}_t)$ using Eq. (2). Further, the fit of the theoretical angular distribution to the measured cross sections, with their associated errors, involves some uncertainty.

Beyond these, the two major sources of uncertainty are the optical model potentials and the choice of bound state wave functions for the transferred nucleon. The latter has been discussed in Sec. IV B. As an indication of the order of magnitude of this uncertainty, we note that using the standard set of binding potential parameters, but increasing r_0 from 1.20 to 1.25 fm for both nuclei, increases the DWBA cross sections, at both high and low energies, almost uniformly by about 25%. Hence the value of the product $(N\tilde{S}_p\tilde{S}_t)$ extracted from the data would decrease by the same amount.

As mentioned in Sec. IV D, optical potentials which give equally good fits to the elastic scattering data at 56 MeV seem to predict the same transfer cross sections to within about 10%. This is no longer true at 352 MeV where, for example (Tables II and III), use of the shallow, surface transparent E-18 type of potential gives cross sections between three and four times larger than those obtained with the A-type of potential.

In these circumstances, one has to appeal to other, independent, information. As discussed in Sec. IV B, this includes shell model predictions of the $\tilde{S}$ factors for the strong transitions, and the results of analyses of light-ion transfer measurements. The various uncertainties associated with these sources probably lead to uncertainties of at least 25% (and maybe much more) in what we can deduce about *absolute* magnitudes from the present experiment. On the other hand, *relative* quantities for the various transitions should be determined much more accurately.

V. RESULTS OF ANALYSES

A. The ^{28}Si(^{18}O,^{17}O)^{29}Si reaction

The DWBA predictions are compared in Fig. 3 with the measured cross sections at 352 MeV for the excitation of states in ^{29}Si accompanied by ^{17}O in its ground state. The corresponding values of the normalization factor $(N\tilde{S}_p\tilde{S}_t)$, relative to the ground state values, are listed in Table II. The angular distributions given by the A- and S-type potentials are almost indistinguishable, and reproduce the shapes of the measured ones quite well. Those obtained from the E-18 type of potential are quite similar,

but with a slight tendency to decrease more rapidly with increasing angle and hence giving a somewhat poorer fit to the data.

The relative values of the normalization factors needed are very similar for all three potentials, certainly within the uncertainties of fitting to the data. They are in quite good agreement with the relative spectroscopic factors obtained from (d,p) measurements[10] for the same $^{28}Si \rightarrow {}^{29}Si$ transitions. Those for the lowest three states are also in good agreement with the predictions of shell model calculations[20] for ^{29}Si, even though there are reasons[28] to believe there is a significant core excitation component in the $\frac{5}{2}^+$ state that would allow it to be excited by a two-step process. (A similar conclusion was reached for the second $\frac{5}{2}^+$ state at 3.07 MeV.) The results for the same reaction measured[7] at 56 MeV show again that the relative spectroscopic factors obtained are insensitive to the choice of optical potential. However, the ratio of the spectroscopic factor needed for the 1.28 MeV $\frac{3}{2}^+$ state to that for the $\frac{1}{2}^+$ ground state, is roughly twice that obtained at 352 MeV. A similar discrepancy, of about 50%, is seen for the same neutron transfers induced[15] by the $^{28}Si(^{15}N,^{14}N)$ reaction at 44 MeV.

There is an apparently similar discrepancy between low and high energy measurements for the $\frac{7}{2}^-$ state at 3.62 MeV; however, the DWBA does not reproduce the angular distributions obtained[7,15] for this transition at the lower energies, suggesting that the theory is neglecting some important feature. For example, this and the $\frac{3}{2}^-$ state at 4.93 MeV are unnatural-parity "intruder" states, perhaps brought down to low excitation energies by collective deformation. The prescription of equating the transfer form factor to the wave function for a single nucleon, bound in a potential well by its separation energy, is probably inadequate in these cases.[1]

In contrast to their relative values, the absolute magnitudes of the DWBA cross sections at 352 MeV are very sensitive to the choice of optical potential, as discussed in Sec. IV D. above. Use of the surface-transparent E-18 type of potential results in spectroscopic factors smaller by factors between 2 and 3 than those obtained using the deep A-type potential. The values of $\tilde{S}_t$ given in Table II were obtained by assuming $N=1$ and taking $\tilde{S}_p=1.6$ for the $^{18}O \rightarrow {}^{17}O_{g.s.}$ transition. Since the standard binding potential parameters were used, the $\tilde{S}_t$ values quoted probably represent upper limits when $\tilde{S}_p=1.6$ is assumed. Comparison with the factors obtained from the (d,p) measurements[10] shows reasonable agreement when the A- or S-type potentials are used; quite small increases in the radial extent of the bound nucleon wave functions, for example, would lead to very good agreement. On the other hand, the comparison implies that the E-18 type of potential yields much too small absolute spectroscopic factors.

This sensitivity to optical potentials does not occur for the same reaction at 56 MeV, or for the $(^{15}N,^{14}N)$ reaction at 44 MeV. At 56 MeV, both the S and E-18 types of potential give absolute spectroscopic factors in agreement with those obtained at 352 MeV when the A- or S-type potentials are used (except for the 1.28 MeV $\frac{3}{2}^+$ state already commented upon), but in severe disagreement with the results obtained with the E-18 potential at 352 MeV. This is another strong argument against the validity of the E-18 type of surface-transparent potential, since the spectroscopic factors should be independent of bombarding energy. The 56 MeV results are also in agreement with the (d,p) measurements, again except for the 1.28 MeV $\frac{3}{2}^+$ state. The $(^{15}N,^{14}N)$ data[15] also gave spectroscopic factors $\tilde{S}_t$ in approximate agreement with the other measurements when $\tilde{S}_p=2.0$ was chosen for the $^{15}N \rightarrow {}^{14}N_{g.s.}$ transition; in this case, the discrepancy for the $\frac{3}{2}^+$ state is less strong.

Some of the differences between the results deduced using a DWBA analysis for different reactions, or at different energies, could arise from multistep processes if the states of ^{29}Si do contain substantial amounts of core excitation.[29] Such contributions, and their interference with the one-step term would vary with energy and the system being studied. A coupled-channels analysis[15] of the $(^{15}N,^{14}N)$ reaction did not appear to lead to any significant changes in the direct ground or $\frac{5}{2}^+$ state spectroscopic factors, although the fits to the angular distributions were improved. A similar analysis[28] of the (d,p) reaction did imply a 35% reduction in the $d_{5/2}$ spectroscopic factors for both $\frac{5}{2}^+$ states. No effect was seen for the 1.28 MeV $\frac{3}{2}^+$ state. Coupled-channels calculations have not been made for the 352 MeV data.

B. The $^{29}Si(^{18}O,^{19}F)^{27}Al$ reaction

The calculated DWBA cross sections are compared in Figs. 4 and 5 to those measured at 352 MeV for transitions to various states in ^{27}Al, with the ^{19}F ejectile left in its 0.199 MeV $\frac{5}{2}^+$ state. The relative normalization factors $N\tilde{S}_p\tilde{S}_t$ and absolute spectroscopic factors are listed in Table III. The absolute values of $\tilde{S}_t$ were obtained by assuming $N=1$ and $\tilde{S}_p=0.41$ for the $^{18}O \rightarrow {}^{19}F_{0.199}$ transition.

Just as for the neutron transfers, all three types of optical potentials give very similar relative cross sections, but the surface-transparent E-18 type results in larger cross section magnitudes than the A or S types by factors of 3 or more. Consequently the $\tilde{S}_t$ values extracted using the E-18 type are smaller by the same factors. They are also much smaller than the $\tilde{S}_t$ predicted by shell model calculations,[20] or those obtained from (d,^{3}He) measurements.[21,22] Since the use of the standard parameter set in Eq. (3) probably results in $\tilde{S}_t$ close to an upper limit, any reasonable variation in these parameters is likely to make the discrepancy worse.

The cross section magnitudes are no longer sensitive to the choice of optical potential at a bombarding energy of 56 MeV. Only two transitions were measured[7] at this energy, both to the ground state of ^{27}Al but leaving ^{19}F in its $\frac{1}{2}^+$ ground state or its $\frac{5}{2}^+$ 0.199 MeV excited state. DWBA calculations with either S-type or E-18 type of optical potentials did not reproduce correctly the observed angular distributions for either transition; the theoretical distributions are peaked at too forward angles. However, fitting to the magnitudes of the peak cross sections gave $\tilde{S}_t \approx 4.1$ when $N=1$ and $\tilde{S}_p$ (g.s.)$=0.21$, $\tilde{S}_p$ (0.199

MeV)=0.41 were assumed, whichever optical potential was used. This is in good agreement with the 352 MeV results when analyzed with the *A*- or *S*-type potentials (Table III), and again provides a strong argument against using the E-18 type of potential at the higher energy.

Proton pickup from ^{28}Si was also studied[15] using the (^{15}N,^{16}O) reaction at 44 MeV. Here the DWBA failed even more dramatically to reproduce the observed angular distributions when optical potentials obtained from scattering analyses were used. They were fitted by a drastic and arbitrary increase in the radius of the real parts of these potentials, thus increasing their refractive power for peripheral collisions. Because of the unknown meaning of this change, the absolute spectroscopic factors extracted are not meaningful; for example, an overall normalization of $N=3.2$ has to be used for the ground state transition to yield the same $\tilde{S}_t=3.76$ as obtained from the (d,^{3}He) reaction.[21] Even the significance of the relative spectroscopic factors is questionable, although they are included in Table III for completeness.

Excitation of the high-spin states at 2.21 MeV ($\frac{7}{2}^+$) and 3.00 MeV ($\frac{9}{2}^+$) in ^{27}Al by a one-step process requires the pickup of a $g_{7/2}$ or $g_{9/2}$ proton, respectively, and hence is strongly inhibited. However, these states probably contain appreciable components of the form $[^{28}\mathrm{Si}(2^+)\otimes 1d_{5/2}^{-1}]$ which can easily be excited by a two-step (inelastic plus transfer) process which is not described by the DWBA. Coupled-channels calculations,[15] using a simplified structure model, for the excitation of these states by the (^{15}N,^{16}O) reaction lend some support to this interpretation. (We note, however, that including these couplings did not remove the difficulties with the angular distributions. An arbitrarily modified optical potential had to be used in the coupled-channels calculations as well.) The 3.0 MeV group corresponds to a doublet which we could not resolve, and probably more than one-half of the cross section is due to exciting the $\frac{9}{2}^+$ member. Hence, we only show DWBA results for the 2.21 MeV group assuming a $1g_{7/2}$ orbital. The corresponding $\tilde{S}_t$ values (Table III) are much larger than the theoretical expectation. This may be due partly to the presence of the two-step excitation just mentioned, and partly because the use of a $1g_{7/2}$ wave function bound with the observed separation energy is unrealistic (Sec. IV B).

According to shell model calculations,[20] the first (1.01 MeV) $\frac{3}{2}^+$ state of ^{27}Al has a very small spectroscopic factor (Table III) for $d_{3/2}$ pickup from the ground state of ^{28}Si, but is easily reached by pickup from the first 2^+ state of ^{28}Si. Thus this transition may be another candidate for excitation by a two-step process. The spectroscopic factors $\tilde{S}_t$ extracted for this state using the DWBA (Table III) are certainly 20 to 30 times larger than the shell model prediction. Without a coupled-channels analysis we cannot say whether this is due to the truncations used in the shell model calculations or to dominant contributions from two-step excitations.

The second $\frac{5}{2}^+$ state at 2.73 MeV in ^{27}Al may also be a candidate for excitation by a two-step process, since the spectroscopic factor predicted[20] for direct pickup is only one-tenth of that for the $\frac{5}{2}^+$ ground state. The observed cross sections (Fig. 5) are an order of magnitude smaller than those for the ground state, but the spectroscopic factors extracted both from the present measurements and from the (d,^{3}He) measurements (Table III) are still a factor of 2 larger than the theoretical values. The results for the third $\frac{5}{2}^+$ state at 4.41 MeV differ even more from the theoretical expectations; it is predicted[20] to have an even smaller spectroscopic factor ($\tilde{S}_t=0.06$), whereas the values needed in a DWBA analysis are an order of magnitude larger ($\tilde{S}_t\approx 0.6$–0.7 for the present measurements).

The sum of the spectroscopic factors $\tilde{S}_t$ obtained for these three $\frac{5}{2}^+$ states is 5.7 for the *A*-type potential and 4.7 for the *S*-type potential. The (d,^{3}He) reaction also yields a sum of 4.7. These sums provide lower limits to the proton occupancy of the $1d_{5/2}$ orbit in ^{28}Si provided the transitions studied are truly direct pickup: see Eq. (1a). The analyses of the 0.84 MeV $\frac{1}{2}^+$ and 1.01 MeV $\frac{3}{2}^+$ states also indicate an occupancy of between 1 and 1.8 for the $2s_{1/2}$ and $1d_{3/2}$ orbits. The total $(2s,1d)$-shell proton occupancy cannot exceed six if the ^{16}O core is not excited. This number is already reached or exceeded by the spectroscopic factors for the transitions reported in Table III. The shell model calculations[20] predict a total occupancy from these transitions of 4.5, with the remaining $(2s,1d)$ strength fragmented among states at higher excitations in ^{27}Al. This may indicate that some part of the observed transition strength is due to two-step or multistep processes, and that the use of the DWBA leads to an overestimate of the empirical spectroscopic factors. On the other hand, the apparent discrepancy is also within the probable errors due to the uncertainties in the various ingredients of the DWBA analyses, as discussed in Sec. IV.

The two odd-parity excitations, to the $\frac{1}{2}^-$ state at 4.05 MeV and the $\frac{3}{2}^-$ state at 5.16 MeV, were analyzed assuming either $1p$ or $2p$ pickup. Similar to the results of the analysis of (d,^{3}He) measurements,[21] using $2p$ wave functions led to spectroscopic factors of about one-quarter of those needed when $1p$ was assumed. In the (^{18}O,^{19}F) analyses reduction factors of 6 and 4 were obtained for the 4.05 and 5.16 MeV transitions, respectively, when using $2p$ instead of $1p$ wave functions. However, as was discussed in Sec. IV B, neither prescription is correct, and a more realistic transfer form factor is required for extracting reliable values. Some difficulty with the assumption of $1p_{1/2}$ for the 4.05 MeV state is already evident from Table III, as the corresponding spectroscopic factors $\tilde{S}_t$ already exhaust the sum rule (1a) for this transition.

VI. SUMMARY AND CONCLUSIONS

We have presented the results of measurements on the single-nucleon transfer reactions ^{28}Si(^{18}O,^{17}O)^{29}Si and ^{28}Si(^{18}O,^{19}F)^{27}Al at a bombarding energy of 352 MeV. Differential cross sections for the most strongly excited residual states were extracted for the angular range $4^\circ\lesssim\theta_{\mathrm{c.m.}}\leq 14^\circ$. Their angular distributions show little structure in this region, being dominated by an exponential decrease with increasing angle. The cross sections at the most forward angles are comparable in magnitude to

the peak cross sections of the bell-shaped angular distributions observed at 56 MeV for the same reactions.

The DWBA to the direct reaction theory of transfer was reviewed, with particular emphasis on the uncertainties involved in its application. The predicted angular distributions are in good agreement with the observed ones. However, because of their lack of structure, they carry no marked signature of the angular momentum transfers involved in each transition or of the spin and parity of the residual state. The *relative* spectroscopic factors extracted agree with those obtained by light ion bombardment of ^{28}Si within the uncertainties of the analyses.

There are theoretical reasons to believe that some of the transitions receive contributions from two-step (inelastic plus transfer) processes. The structureless nature of the angular distributions does not provide any indication of the presence of such processes, so arguments about them must be based upon the magnitudes of the cross sections.

One important result is that the theoretical cross sections at 352 MeV are too large by factors of about 3 when surface-transparent optical potentials of the E-18 type are used. On the other hand, more conventional and deeper potentials, which also fit the observed elastic scattering at this energy, give slightly better fits to the observed transfer angular distributions and also yield the correct magnitudes for the cross sections. We conclude that the E-18 type of potentials are not acceptable at this energy.

A reanalysis of the transfer data obtained at the much lower energy of 56 MeV showed that both types of optical potential give equally acceptable fits to the data with very similar spectroscopic factors. Consequently, the use of the E-18 type of potentials entails energy-dependent spectroscopic factors, whereas use of the other type of potentials does not. This is another strong reason for rejecting the E-18 type of potentials.

The values of the spectroscopic factors extracted also depend upon the assumptions made about the radial wave functions of the transferred nucleon. There is overall agreement between the empirical values and the expectations from the shell model for the transitions to the ground and first excited states of the residual nuclei when a Woods-Saxon binding potential with the standard set of parameters listed in Eq. (3) is used. We conclude that this represents a good choice. However, this prescription for generating transfer form factors is not reliable for the odd-parity states, or for the high-spin states ($I > \frac{5}{2}$). More realistic form factors are required in order to extract meaningful spectroscopic factors for these transitions.

The DWBA failed to reproduce correctly the angular distributions for proton transfer measured at low energies, unless an arbitrary change in the optical potentials was made. The simple, basically exponential, nature of the angular distributions obtained at 352 MeV make it difficult to know whether there is any similar discrepancy at this energy. The DWBA gives the correct slope in the observed angular region, but one could not rule out some shift in angle that might only become apparent if data were available at smaller angles ($\theta_{\text{c.m.}} \lesssim 4°$).

Overall, it appears that the DWBA is able to give the correct absolute and relative magnitudes of the cross sections for both proton and neutron transfers, provided reasonable choices are made for the various ingredients of the theory. Studying the structure of the calculations shows that the contributions from unnatural parity l transfers are important at 352 MeV; hence it is vital to use a theory that includes recoil effects correctly. These contributions are negligible at low energies. By studying the contributions from various partial waves, we also learn that the transfers take place when the two ions are separated by at least 6 fm, with the maximum probability occurring at about 8 fm. This is about 1 fm closer than occurs at a bombarding energy of 56 MeV.

This research was sponsored by the U.S. Department of Energy, under Contract DE-AC05-840R21400 with Martin Marietta Energy Systems, Inc.

[1]G. R. Satchler, *Direct Nuclear Reactions* (Oxford University Press, Oxford, 1983).

[2]W. Henning, Y. Eisen, J. R. Erskine, D. G. Kovar, and B. Zeidman, Phys. Rev. C **15**, 292 (1977).

[3]S. C. Pieper, M. H. Macfarlane, D. H. Gloeckner, D. G. Kovar, F. D. Becchetti, B. G. Harvey, D. L. Hendrie, H. Homeyer, J. Mahoney, F. Puhlhofer, W. von Oertzen, and M. S. Zisman, Phys. Rev. C **18**, 180 (1978).

[4]C. Olmer, M. Mermaz, M. Buenerd, C. K. Gelbke, D. L. Hendrie, J. Mahoney, D. K. Scott, M. H. Macfarlane, and S. C. Pieper, Phys. Rev. C **18**, 205 (1978).

[5]T. J. Humanic, H. Ernst, W. Henning, and B. Zeidman, Phys. Rev. C **26**, 993 (1982).

[6]B. L. Burks, M. A. G. Fernandes, D. J. Horen, G. R. Satchler, R. L. Auble, F. E. Bertrand, J. L. Blankenship, J. L. C. Ford, E. E. Gross, D.C. Hensley, R. O. Sayer, D. Shapira, and T. P. Sjoreen, submitted to Phys. Rev. C.

[7]B. T. Kim, A. Greiner, M. A. G. Fernandes, N. Lisbona, K. S. Low, and M. C. Mermaz, Phys. Rev. C **20**, 1396 (1979).

[8]M. V. Hynes, J. L. C. Ford, Jr., T. P. Sjoreen, J. L. Blankenship, and F. E. Bertrand, Nucl. Instrum. Methods **224**, 89 (1984).

[9]T. P. Sjoreen, J. L. C. Ford, Jr., J. L. Blankenship, R. L. Auble, F. E. Bertrand, E. E. Gross, D. C. Hensley, D. Schull, and M. V. Hynes, Nucl. Instrum. Methods **224**, 421 (1984).

[10]M. C. Mermaz, C. A. Whitten, Jr., J. W. Champlin, A. J. Howard, and D. A. Bromley, Phys. Rev. C **4**, 1778 (1971).

[11]L. L. Green, C. O. Lemon, and I. M. Nagib, Nucl. Phys. **A142**, 137 (1970); C. Schmidt and H. H. Duhm, *ibid.* **A155**, 644 (1970).

[12]H. H. Macfarlane and S. C. Pieper, Argonne National Laboratory Report No. ANL-76-11, 1978 (unpublished).

[13]R. M. DeVries, G. R. Satchler, and J. G. Cramer, Phys. Rev. Lett. **32**, 1377 (1974).

[14]R. M. DeVries, Phys. Rev. C **8**, 951 (1973).

[15]J. C. Peng, B. T. Kim, M. C. Mermaz, A. Greiner, and N. Lisbona, Phys. Rev. C **18**, 2179 (1978).

[16]G. R. Stachler, Nucl. Phys. **A329**, 233 (1979).

[17]T. K. Li, D. Dehnhard, R. E. Brown, and P. J. Ellis, Phys. Rev. C **13**, 55 (1976).

[18]J. B. McGrory and B. H. Wildenthal, Phys. Rev. C **7**, 974 (1973).
[19]L. L. Lee, J. P. Schiffer, B. Zeidman, G. R. Satchler, R. M. Drisko, and R. H. Bassel, Phys. Rev. **136**, B971 (1964).
[20]B. H. Wildenthal and J. B. McGrory, Phys. Rev. C **7**, 714 (1973).
[21]B. H. Wildenthal and E. Newman, Phys. Rev. **167**, 1027 (1968).
[22]H. E. Gove, K. H. Purser, J. J. Schwartz, W. P. Alford, and D. Cline, Nucl. Phys. **A116**, 369 (1968).
[23]W. T. Pinkston, R. J. Philpott, and G. R. Satchler, Nucl. Phys. **A125**, 176 (1969).
[24]G. C. Li, M. R. Yearian, and I. Sick, Phys. Rev. C **9**, 1861 (1974).
[25]F. Pougheon and P. Roussel, Phys. Rev. Lett. **30**, 1223 (1973); W. von Oertzen, Phys. Lett. **151B**, 95 (1985).
[26]W. A. Friedman, K. W. McVoy, and G. W. T. Shuy, Phys. Rev. Lett. **33**, 308 (1974).
[27]R. A. Broglia and A. Winther, *Heavy Ion Reactions* (Benjamin-Cummings, Reading, Mass., 1981), Vol. 1, p. 184.
[28]W. E. Frahn, in *Heavy-ion Science,* edited by D. A. Bromley (Plenum, New York, 1984) Vol. 1; *Diffractive Processes in Nuclear Physics* (Oxford University Press, Oxford, 1984).
[29]W. R. Coker, T. Udagawa, and G. W. Hoffman, Phys. Rev. C **10**, 1792 (1974).